Structures of self-assembled amphiphilic peptide-heterodimers: effects of concentration, pH, temperature and ionic strength†

Zhongli Luo,[a] Björn Åkerman,[a] Shuguang Zhang[b] and Bengt Nordén*[a]

Received 22nd December 2009, Accepted 2nd March 2010
First published as an Advance Article on the web 8th April 2010
DOI: 10.1039/b926962b

The amphiphilic double-tail peptides AXG were studied regarding secondary structure and self-assembly in aqueous solution. The two tails A = Ala_6 and G = Gly_6 are connected by a central pair X of hydrophilic residues, X being two aspartic acids in ADG, two lysines in AKG and two arginines in ARG. The peptide AD (Ala_6Asp) served as a single-tail reference. The secondary structure of the four peptides was characterized by circular dichroism spectroscopy under a wide range of peptide concentrations (0.01–0.8 mM), temperatures (20–98 °C), pHs (4–9.5) and ionic strengths. In salt-free water both ADG and AD form a β-sheet type of structure at high concentration, low pH and low temperature, in a peptide–peptide driven assembly of individual peptides. The transition has a two-state character for ADG but not for AD, which indicates that the added tail in ADG makes the assembly more cooperative. By comparison the secondary structures of AKG and ARG are comparatively stable over the large range of conditions covered. According to dynamic light scattering the two-tail peptides form supra-molecular aggregates in water, but high-resolution AFM-imaging indicate that ordered (self-assembled) structures are only formed when salt (0.1 M NaCl) is added. Since the CD-studies indicate that the NaCl has only a minor effect on the peptide secondary structure we propose that the main role of the added salt is to screen the electrostatic repulsion between the peptide building blocks. According to the AFM images ADG and AKG support a correlation between nanofibers and a β-sheet or unordered secondary structure, whereas ARG forms fibers in spite of lacking β-sheet structure. Since the AKG and ARG double-tail peptides self-assemble into distinct nanostructures while their secondary structures are resistant to environment factors, these new peptides show potential as robust building blocks for nano-materials in various medical and nanobiotechnical applications.

Introduction

The self-assembly processes where peptide chains fold into proteins or when single-stranded DNA forms helical duplexes by base-pairing have recently been employed to design and fabricate a wide range of nanomaterials[1,2] that may meet diverse applications.[3–5] In the same vein the self-assembly of lipids into cell membranes inspired Zhang and co-workers to study how lipid-like oligo-peptides can form new materials in water.[6–9] The peptides were designed to have a single chain of hydrophobic amino acids as a tail, connected to a hydrophilic head consisting of one or two amino acids, as in A_6D, A_6K, V_6D, V_6K, G_4D_2, G_6D_2, G_8D_2 and L_6D_2 (using standard one-letter abbreviations for the amino acids). Once dissolved in water these peptides[6–9] have similar properties as commonly used amphiphilic substances such as *n*-dodecyl-beta-D-maltoside (DM) and octyl-D-glucoside (OG). Designed amphiphilic molecules can be useful as evidenced by the use of polymers, lipids, surfactants and detergents in applications ranging from DNA binding to DNA release and gene therapy.[10–16] In gene transfer applications oligo-peptides are often designed starting from naturally occurring peptides that catalyze transport across membrane bilayers, such as the linear oligopeptide penetratin.[17,18] Synthetic surfactants such as DM and OG have been used to stabilize proteins in solution or crystal,[19,20] but already small and structurally simple self-assembling peptides such as A_6K and V_6D have been shown to stabilize some membrane proteins including Photosystem I[21] and GPCR bovine rhodopsin.[22] One *de novo* approach to prevent membrane proteins from aggregating in aqueous solution is thus to design new peptide sequences. Considering how many oligo-peptide variants may be synthesized by solid phase chemistry, designed peptides may be a more fruitful approach than conventional organic chemistry for rational design of surfactants for membrane protein crystallization and other applications.

Our present strategy is to expand the single-tail theme of the surfactant-mimics A_6Z (where Z = K or D) by adding a second tail on the C-terminus side, in order to form two-tail peptides of the class $A_6Z_2G_6$ which we shall denote AXG. The central residue pair $X = Z_2$ will serve as a hydrophilic "head" at pH 7, since the aspartic acid (Z = D in ADG) carries a negative charge while lysine (Z = K in AKG) and arginine (Z = R in ARG) will be positively charged. Notably, the two tails A = $(Ala)_6$ and G = $(Gly)_6$ (Scheme 1) contain different amino acid residues. The

[a]*Department of Chemical and Biological Engineering, Chalmers University of Technology, Gothenburg, SE-41296, Sweden. E-mail: Norden@chalmers.se; Zhongliluo@163.com; Fax: +46 31 772 3858; Tel: +46 31 772 3041; +46 31 772 3056*
[b]*Center for Biomedical Engineering and Center for Bits and Atoms, NE47-379, Massachusetts Institute of Technology, Cambridge, MA, 02139-4307, USA*

† Electronic supplementary information (ESI) available: Peptide charge *vs* pH, Effect of pH and charge on CD-amplitudes. See DOI: 10.1039/b922426b

corresponding homo-dimeric peptides AXA are being investigated in a separate study (Zhongli Luo, to be published).

A long-term goal is to find applications of the two-tail peptides by exploiting their tendency to self-assemble in water. Since previous results[5] suggest that self-assembly of oligo-peptides is strongly influenced by their secondary structure, our first goal was to use circular dichroism to investigate how peptide concentration, pH and temperature affect the secondary structure of the double-tailed peptide building blocks, using A_6D as a single-tail reference. These CD-studies were performed in pure water (no added salt), with the goal to capture the peptide conformation before the self-assembly was initiated by increasing the ionic strength.[2] Dynamic light scattering (DLS) was used to study the size distribution of the four oligo-peptides in pure water before the salt was added. Atomic force microscopy (AFM) was used to investigate the final outcome once the self-assembly was initiated by adding salt, using AFM-imaging in salt-free water as a control.

Materials and methods

Peptide synthesis, purification and properties

The primary structures of the four peptides (including end-modifications) are shown in Scheme 1, and Table 1 summarizes other properties. The parts $(Ala)_6$ and $(Gly)_6$ will be referred to as "tails", while the central pair of residues (Z_2 with Z = Asp, Lys or Arg) is the "head".

The peptides were custom-made by solid-phase synthesis (ADG and ARG, Shanghai Science Peptide Biotech. Co., Ltd, China; AKG, CPC, Scientific Inc., CA, USA; AD from MIT, S. Zhang lab), including the capping by acetylation at the N-terminus and amidation at the C-terminus. Purified by HPLC and characterized by mass spectroscopy, the peptide purities were 99.4% for ADG, 96.3% for ARG and 84.6% for AKG, while the purity of AD was considerably lower (~80%). Stock solutions of concentration 10 mM peptide (ADG, ARG and AKG) were prepared by dissolving the peptides in water (Millipore Milli-Q system), and were stored at 4 °C before use.

Molecular modeling

Fig. 1 shows the four amphiphilic peptides in two possible conformations, β-sheet and α-helix, as constructed by using the modeling software Hyperchem professional version 7.5. The structures have not been energy-minimized, and are only meant to provide a picture of the relative size of the tails and the head, and the relative positions of the side groups in the two amino acids of the head.

ADG:
Ac-Ala-Ala-Ala-Ala-Ala-Ala-Asp-Asp-Gly-Gly-Gly-Gly-Gly-Gly- $CONH_2$

AKG:
Ac-Ala-Ala-Ala-Ala-Ala-Ala-Lys-Lys-Gly-Gly-Gly-Gly-Gly-Gly- $CONH_2$

ARG:
Ac-Ala-Ala-Ala-Ala-Ala-Ala-Arg-Arg-Gly-Gly-Gly-Gly-Gly-Gly-$CONH_2$

AD:
Ac-Ala-Ala-Ala-Ala-Ala-Ala-Asp-$CONH_2$

Scheme 1 Primary structure of the peptides.

The carboxylic groups in ADG are closer to each other than the amine groups in AKG, irrespective of the secondary structure (Fig. 1), in accordance with the pK_a-values of ADG being further apart than for AKG (Table 1). Similarly, the molecular modeling indicates that the guanidium groups in ARG are approximately as far apart as the amine groups are from each other in AKG, so the two pK_a-values of ARG are expected to be roughly the same, within one pH-unit, as is the case with AKG. In Table 1 we assume they are equal to free Arg. Fig. S1 (see ESI†) shows the calculated net charges of the peptides *vs.* pH, taking into account that the end-groups are expected to be pH-inactive in water because of their amide-caps.[23,24]

Circular dichroism (CD) spectroscopy

CD spectra between 190 and 260 nm were recorded on a Jasco-810 spectrometer (Jasco Corp, Japan). The CD amplitude was converted to an average ellipticity [θ] per residue (given in deg cm^2 $dmol^{-1}$) by using

$$[\theta] = \text{mdeg}/([\text{peptide}] \times l \times n \times 10)$$

where l is the optical path length (cm), n is the number of amino acid residues in each of the peptides and [peptide] is molar concentration (M) of peptide. Combining established interpretations of protein spectra in near UV[25] with conclusions from recent far-UV studies[26,27] the CD spectra were assigned as β-sheet (negative minimum at about 216 nm, positive maximum at 195–200 nm), α-helix (negative band split between two peaks at 210 and at 225 nm, a positive peak at about 195 nm with about twice the residue-ellipticity compared to the β-sheet maximum) or "other" (such as "turns" and "unordered"). Interpretation of the CD spectra was sometimes assisted by decomposition into contributions from α-helix, β-sheet, turns and unordered structures by using the program CONTIN from the DichroWeb (http://dichroweb.cryst.bbk.ac.uk/html/home.shtml) courtesy of Professor B. Wallace. There was substantial scatter in the CD-data below 195 nm in some cases (probably caused by too high sample absorption), and these data points have not been included in the analysis.

Using 200 μL of sample in a 0.1 cm path length cuvette, the peptide concentrations varied between 0.01 and 1.0 mM by diluting the stock solutions (10 mM), using milliQ-water if not otherwise stated. The temperature was controlled within 1 °C using an external heat bath. In temperature scans the samples were examined by increasing or decreasing temperature between 20 and 98 °C in increments of 2 °C and allowing a 30-second equilibration time at each temperature. The effect of pH was investigated by equilibrating the samples for 2 hours in phosphate buffer at the desired pH as adjusted by HCl or NaOH. When the peptides are dissolved in pure water (no buffer) the estimated pH (using the pK_a-values in Table 1) is 3.5 for 0.5 mM ADG, 3.6 for AD, 10.8 for AKG and 11.8 for ARG. Self-assembly of the peptides was initiated at room temperature either by adding NaCl (as an equal volume of 0.2 M NaCl, giving a final concentration of 0.1 M) or by incubation in PBS solution

Table 1 Peptide properties

	Primary structure[a]	M_w (Da)	pK_{a1}[b]	pK_{a2}[b]	Charge at pH 7	L[c] (nm)	D_1[d] (nm)	D_2[d] (nm)
ADG	$A_6D_2G_6$	1058	3.40[e] (ref. 37)	4.70[e] (ref. 37)	−2	2–5	85 ± 7 (50%)	130 ± 50 (50%)
AKG	$A_6K_2G_6$	1084	10.05[f] (ref. 38)	11.01[f] (ref. 38)	+2	2–5	250 ± 100	—
ARG	$A_6R_2G_6$	1140	12.5[g]	12.5[g]	+2	2–5	150 ± 50 (30%)	450 ± 200 (70%)
AD	A_6D	600	4.0[h]	—	−1	1–2.5	200 ± 100	—

[a] Using one-letter abbreviations for the amino acids. See Scheme 1 for molecular structures. [b] Dissociation constants for the side-chains of the central residue-pairs (D_2, K_2, R_2). The N- and C-terminal groups are protolytically inactive due to the amide-capping (see Scheme 1). [c] Maximum length between the N- and C-terminal of the individual peptides from molecular modeling of α-helix and β-sheet by Hyperchem professional version 7.5. [d] Average dimension of aggregates formed in water as measured by DLS (Fig. 8). In case of bimodal distributions the values in parenthesis give the percentages of the two size-contributions. [e] Using the pK_a-values of the Asp–Asp dimer aspartyl–aspartic acid.[37] [f] Using the pK_a-values of the Lys–Lys dimer lysyl–lysine.[38] [g] Assumed to be the same as for free Arg, since the diprotic properties of the Arg–Arg dimer have not been investigated to our knowledge. [h] The monoprotic AD is assumed to have the same pK_a as free Asp.

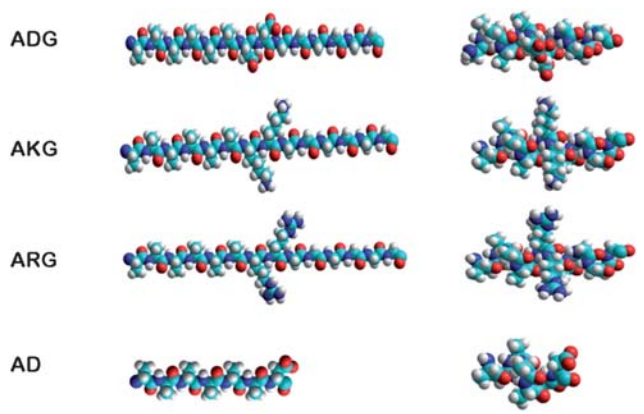

Fig. 1 Proposed β-sheet (left) and α-helix (right) conformations of each of the four peptides, with double tails and a central head according to Scheme 1, as obtained by molecular modelling. The structures are not energy minimized, and only meant as guidance to judge relative sizes and approximate distances between protolytic groups in the two central residues. The N-terminus is at the left, and the atoms are color-coded as: hydrogen = white, carbon = cyan, oxygen = red and nitrogen = blue.

(0.058 M Na_2HPO_4, 0.017 M NaH_2PO_4, 0.069 M NaCl, 2 mM Mg^{2+}, pH = 7.2). Considering that the peptide solutions are dilute, we have used the Jasco spectral analysis software to correct the baseline for the 0.01 mM peptide solutions.

Dynamic light scattering (DLS)

Dynamic light scattering experiments were performed at 25 °C with DTS (nano, Malvern, UK) on 200 μL aliquots of the 0.5 mM peptide solutions. The Precision DTS program was used for evaluating the hydrodynamic size and plotting the fractional distribution *versus* size. Each peptide type was studied in three independent measurements on freshly prepared samples, and in each of the three cases the distribution curves were based on the average of 10 correlation curves. Only size-distributions with polydispersity index (PDI) below 0.56 were used in the presented average size distributions.

Atomic force microscopy (AFM)

The same samples used in DLS were incubated in 0.1 M NaCl solution overnight at an approximate peptide concentration of 0.25 mM. Aliquots of 2–5 μL were deposited onto a freshly cleaved mica surface. To optimize the amount of peptide adsorbed, each aliquot was left on the mica surface for 30–60 seconds and then washed with 1000 μL deionized water at least three times. The mica surface with the adsorbed peptide was then dried in air and imaged immediately. The images were obtained by scanning the mica surface in air by AFM (NT-MDT, Russia) operating in Tapping Mode. Soft silicon cantilevers with spring constant 1–5 N m^{-1} and tip radius of curvature of 5–10 nm (NSG-01,NT-MDT, Russia) were chosen in order to minimize the tip tapping force and optimize the resolution in the imaging of the soft biopolymers. AFM scans were taken at 512 × 512 pixels resolution and produced topographic images of the samples, in which the brightness of features increases as a function of height. Typical scanning parameters were as follows: scan mode: Simul, data type: topography, area/speed from 100 × 100 μm to 1000 × 1000 nm/0.5–1.5 Hz, amp. ref.: −0.1 to −0.3, vib. voltage: 1.0–2.0 V, bias: 0.000 V, integral and proportional gains: 0.05–0.2 and 0.1–0.5 respectively. Notably, the molar peptide concentrations in AFM (0.1–10 mM) overlap with the concentration range in the CD studies (0.01–0.8 mM peptide).

Results

A. Peptide secondary structure before self-assembly

Circular dichroism (CD) spectroscopy was used to monitor how the secondary structure of the oligo-peptides in water is affected by peptide concentration, pH and temperature, as well as ionic strength. Based on their shape the CD spectra were assigned as β-sheet, α-helix, turns or unordered[27] (see Materials and methods).

Effect of peptide concentration on secondary structure. Fig. 2 shows the CD spectra of the peptide ADG at various concentrations when dissolved in pure water (no buffer or added salt). As expected the CD amplitude increases with increasing peptide concentration. However, also the spectral shape is affected by the peptide concentration, as shown by a plot of the corresponding average ellipticity [θ] per residue for ADG (Fig. 3a). At high concentration ADG (0.8 mM) has the bisignate shape characteristic of a β-sheet (minimum at 218 nm, maximum at 204 nm), so the distinctly different shape of the CD-spectrum at 0.1 mM indicates a different secondary structure at low concentrations. The isodichroic point at 214 nm for the ADG-spectra between

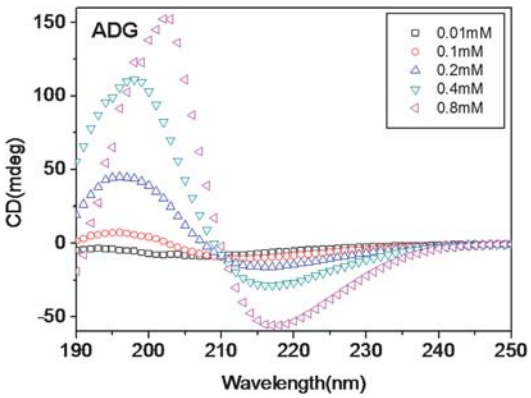

Fig. 2 CD-spectra of ADG (see Scheme 1) at indicated concentrations (mM peptide) dissolved in water at 25 °C.

0.1 and 0.8 mM suggests a two-state conversion from a low concentration secondary structure into a β-sheet as the ADG concentration is increased. The ellipticity-amplitude of the high-concentration conformation ($[\theta] = -12\,500$ deg cm^2 dmol^{-1} at 218 nm) is about 2 times lower than reported for the mixed sequence peptide EAK16 ($[\theta] = -22\,000$ deg cm^2 dmol^{-1}).[2]

Fig. 3b–d show the CD spectra of the other three peptides in the same range of peptide concentrations. The behavior of the single tail control AD (Fig. 3d) is similar to that of ADG, including a β-sheet spectrum characteristic at the highest concentration, even though the isodichroic point seen with ADG is notably absent for AD. By contrast the CD spectra of both AKG (Fig. 3b) and ARG (Fig. 3c) are dominated by a single negative band centered at about 200 nm, indicating that both peptides deviate from a β-sheet secondary structure. Fig. 4 shows the CD-spectra of the four peptides measured at a highly diluted concentration (0.01 mM) with the aim to investigate the secondary structure of the individual peptide building blocks. All four peptides are seen to exhibit a single negative CD band at low

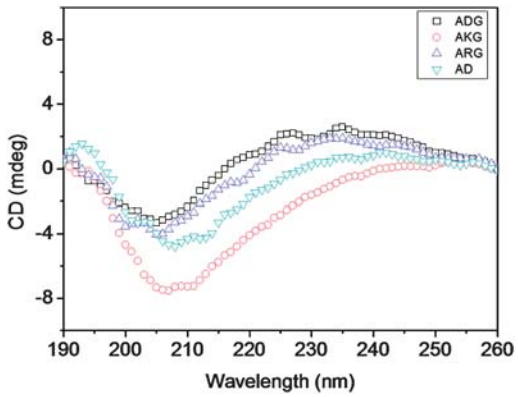

Fig. 4 CD spectra of the indicated peptides under dilute conditions. Peptide concentration: 0.01 mM dissolved in water at 25 °C.

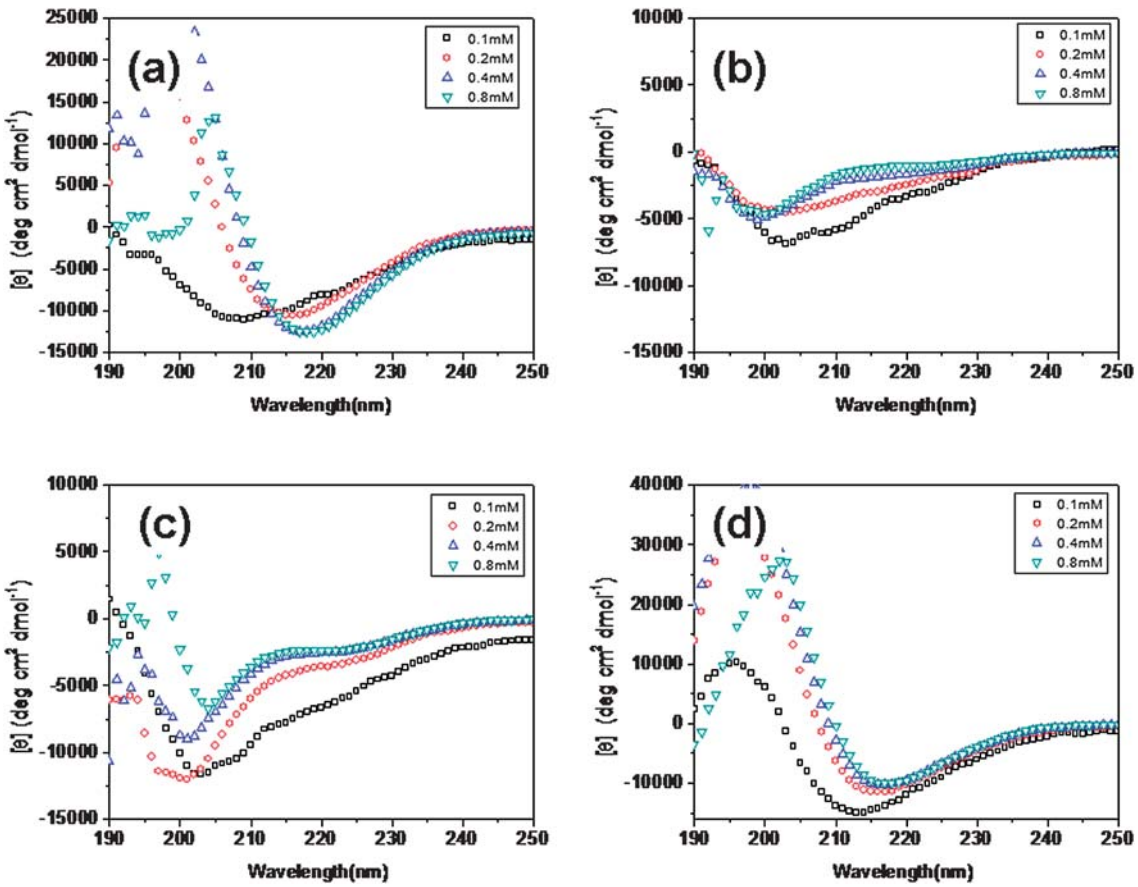

Fig. 3 Molar CD spectra of (a) ADG, (b) AKG, (c) ARG and (d) AD at the indicated concentrations (mM peptide) dissolved in water at 25 °C.

concentrations, with a spectral shape that is notably similar considering how different the spectra are at higher concentrations (Fig. 3). This observation suggests that the four peptides attain a similar (albeit unknown) conformation under dilute conditions, and that peptide–peptide interactions induce a secondary structure at higher concentrations which depends on the primary structures of the peptides.

Effect of pH on secondary structure. Fig. 5 shows how the CD-spectra of the four peptides depend on pH between 4.0 and 9.5, in solutions containing 0.2 mM peptide. At pH 4 both ADG (Fig. 5a) and AD (Fig. 5d) exhibit the bisignate CD spectrum of a β-sheet (minimum at 216 nm and a maximum at 198 nm). The CD-amplitudes are seen to decrease with increasing pH for both peptides, which indicate that the lower the amount of β-sheet structure in ADG and AD the higher the pH. Other secondary structures thus appear at high pH, and as in Fig. 3 there is an isodichroic point for ADG (now at 208 nm) but not for AD. By contrast, the spectral shapes for the AKG (Fig. 5b) and ARG (Fig. 5c) peptides are essentially unaffected by pH between 4.0 and 9.5, indicating that they do not undergo a secondary structure transition in this pH-range.

Effect of temperature on secondary structure. Fig. 6 shows how the CD-spectra of the four peptides depend on the temperature. With increasing temperature, the ADG-spectra (Fig. 6a) exhibit a transition from a characteristic β-sheet spectrum towards an unordered type of spectrum. Again ADG exhibits an isodichroic point (at 210 nm) which appears to be absent for AD (Fig. 6d). By comparison, the CD spectra of AKG (Fig. 6b) and ARG (Fig. 6c) are essentially the same between 20 and 98 °C which supports that the secondary structures of these two peptides are unusually stable towards changes in temperature (Fig. 6) as well as concentration (Fig. 3) and pH (Fig. 5). However, since the CD-spectra in Fig. 6b (and 6c) indicate an unordered type of secondary structure, one cannot exclude the possibility that AKG (and ARG) attains different types of unordered structures at different temperatures.

B. Peptide aggregation and self-assembly

Sizes of supramolecular aggregates formed in water. To assess the potential of double-tail peptides to form supramolecular structures we performed DLS experiments to measure the size-distribution of the four peptides in aqueous solution. The presented data (Fig. 7) are in pure water, that is, before the addition of salt to initiate self-assembly. In the presence of salt (0.1 M NaCl) the peptide-complexes turned out to be too large to study by DLS, so AFM was used instead (see below). The DLS-data in salt-free water (Fig. 7) show wide size-distributions that are

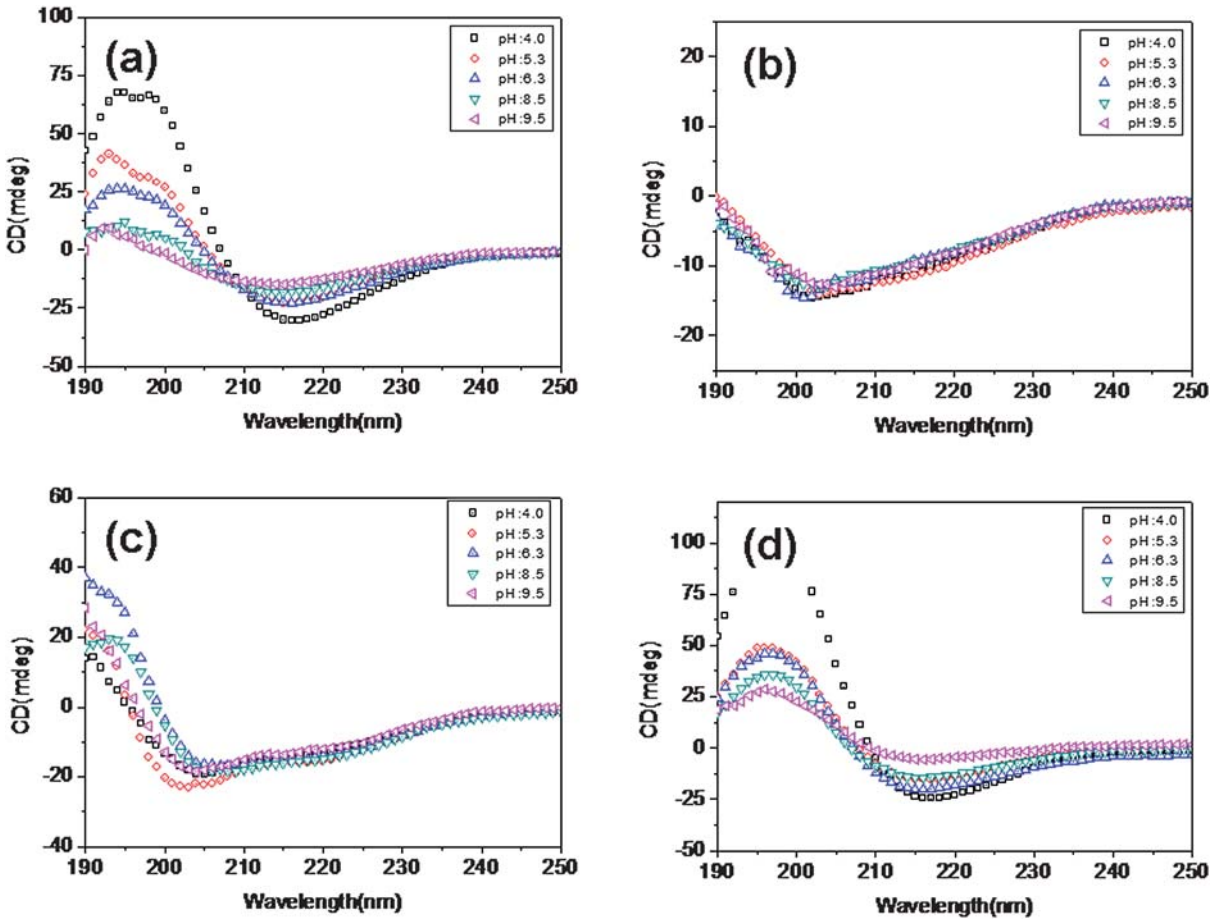

Fig. 5 Effect of pH on secondary structure. CD spectra of (a) ADG, (b), AKG, (c) ARG and (d) AD at the indicated pH-values. Peptide concentration: 0.2 mM and temperature: 25 °C.

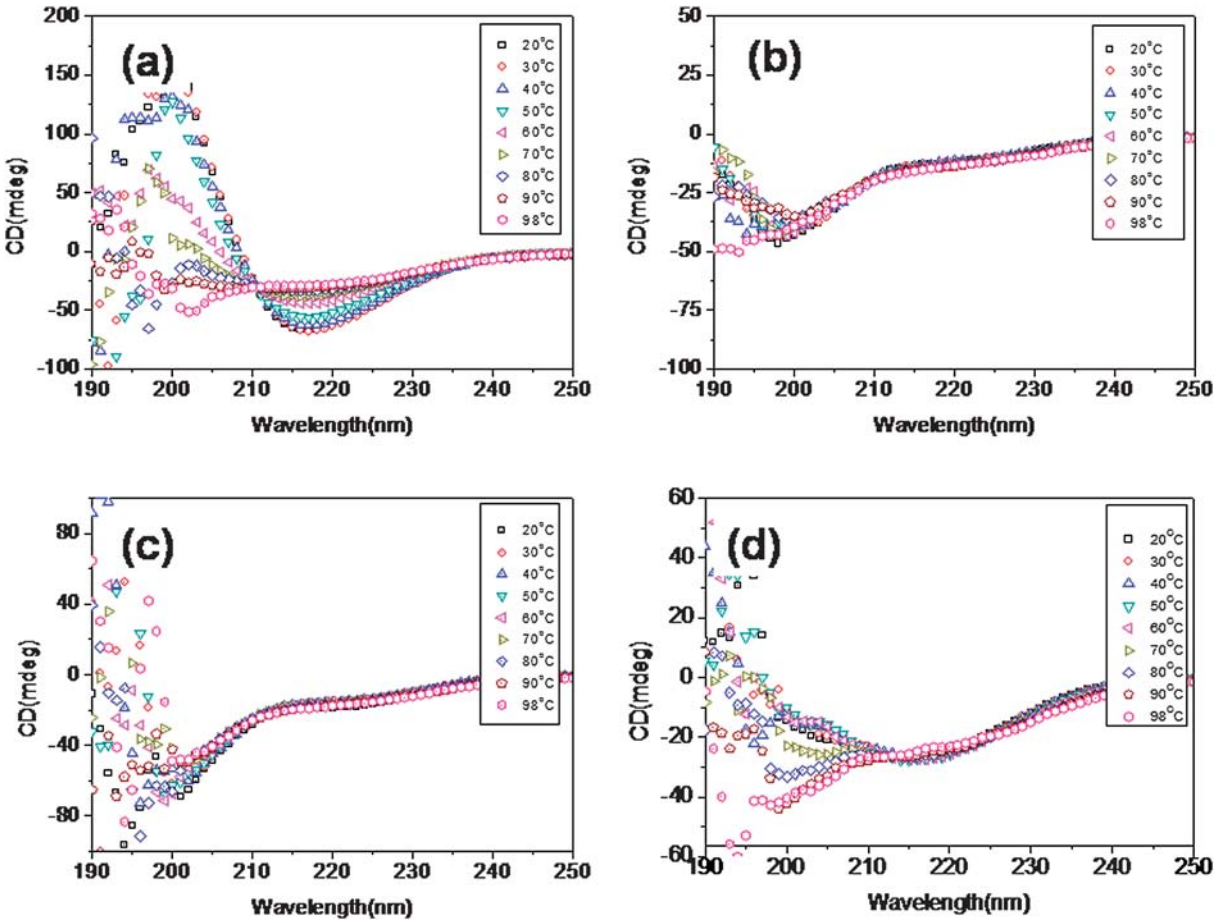

Fig. 6 Effect of temperature on secondary structure. CD spectra of (a) ADG, (b) AKG, (c) ARG and (d) AD at the indicated temperatures. Peptide concentration: 0.5 mM dissolved in water.

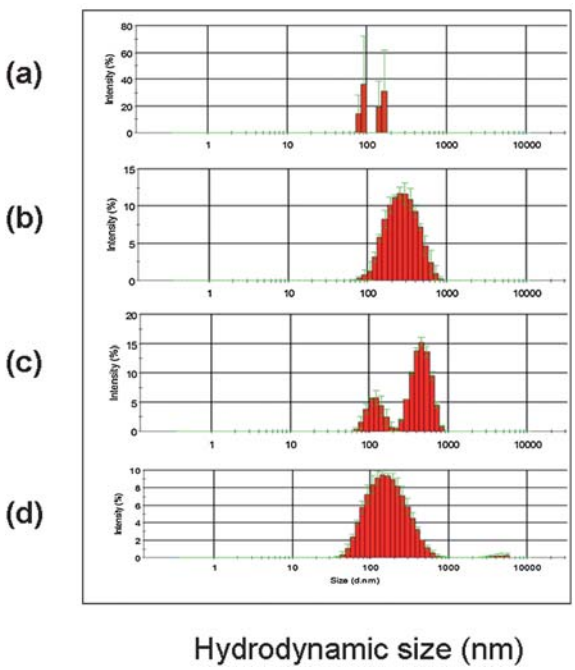

Fig. 7 DLS-data on the size-distributions of the supra-molecular aggregates formed in water by (a) ADG, (b) AKG, (c) ARG and (d) AD at 25 °C. Peptide concentration: 0.5 mM.

reproducibly non-monomodal for ADG and ARG but bimodal for AKG and AD. The average sizes of the structures that the four peptides form in water are given in Table 1, and it is notable that the typical sizes are much larger than for the individual peptides (Table 1). The polydispersity index ranged from about 0.20 (AD) to 0.56 (AKG), with a variation of 0.06 or smaller for a given peptide.

The effect of added salt on peptide secondary structure. Peptide self-assembly is often initiated by adding salt,[2] so ions appear to play an important role in this process. Fig. 8 shows how the secondary structure of the four peptides (as monitored by CD) is affected by adding either 0.1 M NaCl or PBS buffer, two salt-solutions chosen to mimic physiological conditions. When incubated in PBS the peptides ADG (Fig. 8a) and AD (Fig. 8d) loose the CD-characteristics of a β-sheet secondary structure, whereas the CD-spectra of AKG and ARG are only weakly affected. In 0.1 M NaCl the peptide AD (Fig. 8d) retains its β-sheet characteristic whereas ADG (Fig. 8a) attains a secondary structure that is somewhat different than in water. The CD spectra of AKG (Fig. 8b) and ARG (Fig. 8c) are essentially unaffected by the addition of NaCl.

High resolution structures after self-assembly. DLS (Fig. 7) can only provide low-resolution structural data on

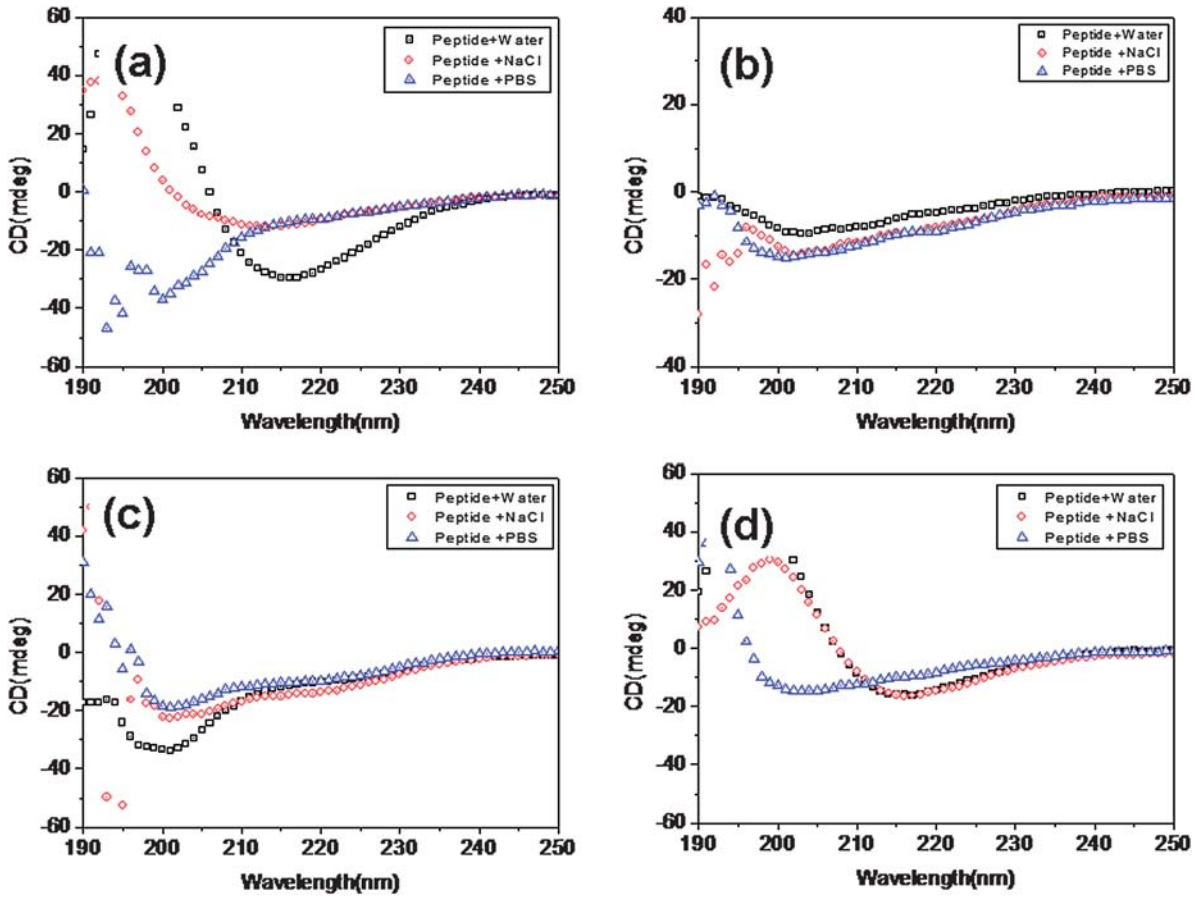

Fig. 8 Effect of added salt on secondary structure. CD spectra of (a) ADG, (b) AKG, (c) ARG and (d) AD at 25 °C under the indicated salt conditions. NaCl (0.1 M NaCl, peptide concentration: 0.2 mM dissolved in water); PBS (pH = 7.2, peptide concentration 0.2 mM) and water (peptide concentration: 0.2 mM dissolved in water; no buffer or added salt).

ensemble-averaged dimensions (Table 1), so we used AFM (Fig. 9) to investigate the nanometre structure of the individual structures that the four peptides form in 0.1 M NaCl solution, using peptides in water with no added salt as a control (right hand panel for each peptide). In the presence of 0.1 M NaCl the peptides form various types of ordered structures that are not observed in the absence of added salt. In addition there are sub-micron particle-like structures seen both with and without added salt. According to the AFM images, ADG (Fig. 9a) typically self-assemble into nanofibers that are about 80 nm wide, 3–5 nm high, and 3500–5000 nm in length. The structures formed by the single-tail control AD (Fig. 9d) are similar to those reported previously,[9] nanofibers approximately 100 nm wide, 2–5 nm high and 3000–5000 nm long. The peptide ARG (Fig. 9c) also self-assembles into nanofibers, about 80–120 nm wide, 3–5 nm high and 5000–8000 nm long. By contrast, the peptide AKG (Fig. 9b) forms nano-layer networks which seem to consist of nanofibers. The combined AFM data suggest that the double tail peptides could self-assemble into nanofibers or nanolayers depending on the peptide primary structure.

The sub-micron particles we observe by AFM have not been analyzed regarding their chemical composition, so we cannot exclude that they contain salt crystals (from the peptide preparations) rather than peptides.

Discussion

Designed peptides have been studied towards applications in materials science, biotechnology and medicine.[5,22,28,29] The peptides investigated here (Scheme 1) differ from those studied previously in two ways. The new peptides have two tails, as opposed to single-tail amphiphilic molecules like A_6K and A_6D.[9] Secondly they have a unique sign of charge as opposed to the alternating positive and negative residues in peptides such as AEK-16,[2] RADA-16[30] and d-EAK16.[31] Our goal was to investigate the potential of these new peptides as building blocks for self-assembly, using CD to follow their secondary structure and DLS and AFM to monitor the supramolecular aggregates that they form in water.

The four peptides attain similar conformations when left to themselves (Fig. 4) and still they form very different supramolecular structures (Fig. 9), but only if the peptide concentration is high enough to affect their secondary structure (Fig. 3). Taken together these observations suggest that not only individual peptides act as building blocks for the self-assembled structures but also that the final outcome depends on their amino acid sequence. One fundamental question is then how the peptide primary structure guides the supramolecular outcome: does the peptide act directly through its designed primary sequence or

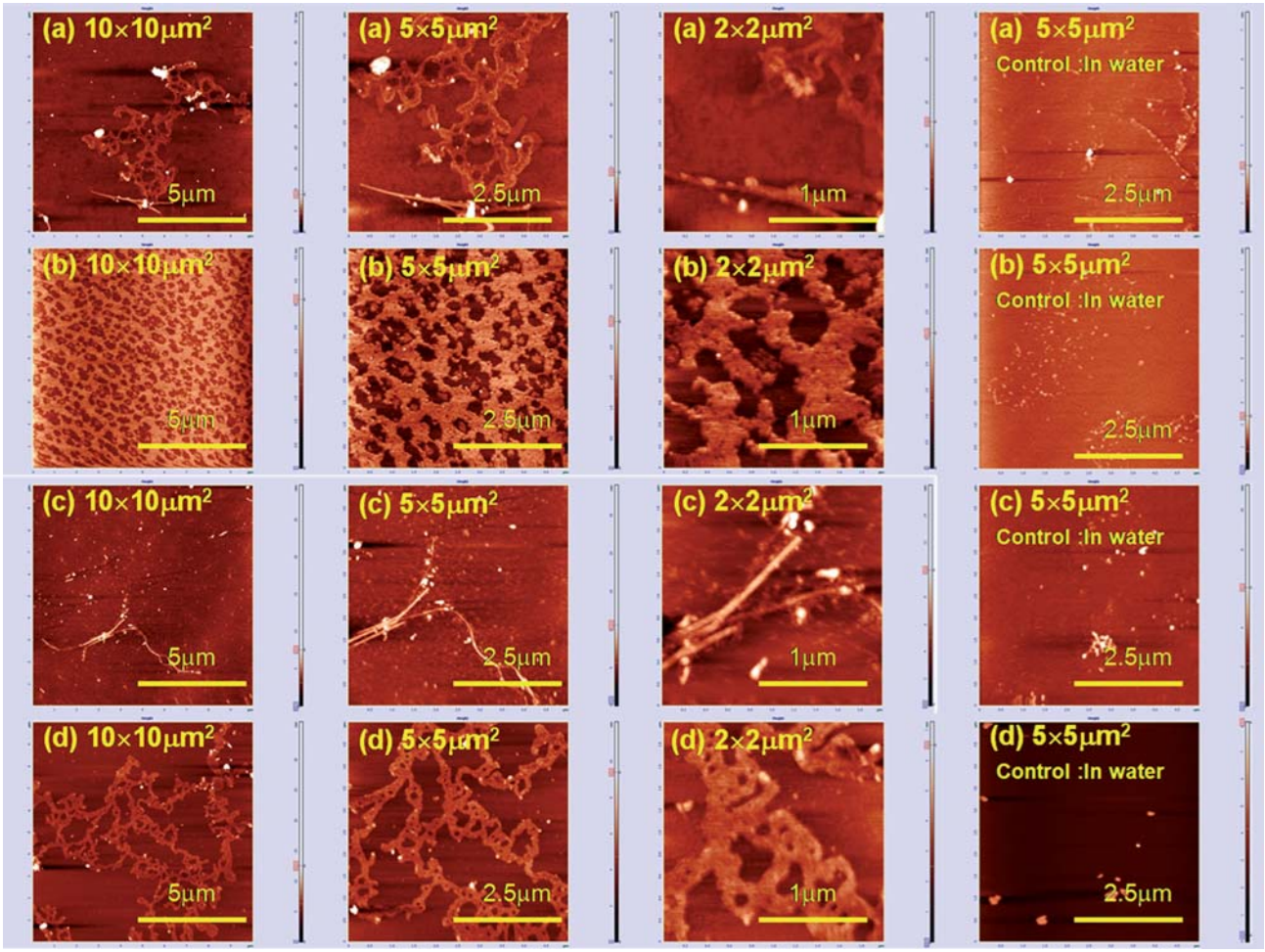

Fig. 9 AFM-images of the structures formed by (a) ADG, (b) AKG, (c) ARG and (d) AD in 0.1 M NaCl, at different degrees of magnification compared to the control in water (no added salt) at 25 °C. Peptide concentration: 250 μM dissolved in water. (See Material and methods for details of sample preparation).

does it control the supramolecular structure indirectly by being more prone to form a certain solvent-induced secondary structure?

Here we address this question by comparing the secondary structure (Fig. 8) and the supramolecular outcome (Fig. 9) in two solvents: pure water and an aqueous solution of 0.1 M NaCl. From Fig. 9 it is clear that adding NaCl leads to an ordered supramolecular structure which cannot be obtained in salt-free water, so it is interesting to investigate how the added NaCl affects the peptide secondary structure.

A. Peptide behavior in pure water

Effects of concentration on secondary structures. In water ADG forms a characteristic β-sheet spectrum at high concentration (Fig. 3a), whereas the conformation at the lowest concentration (Fig. 4) probably is α-helix (according to CONTIN-analysis; see Materials and methods). The conversion between the two conformations most likely occurs in a two-state process, since ADG displays an isodichroic point when the peptide concentration is increased. The single-tail control AD also exhibits a characteristic β-sheet spectrum at high enough concentration (Fig. 3d), but the transition from the low-concentration structure is less distinct since the CD spectra lack an isodichroic point. A pattern of two-state behavior for ADG, but not for AD, also emerges from the CD spectra at increasing pH (Fig. 5) or temperature (Fig. 6), since in both cases an isodichroic point is observed with ADG but not with AD. The difference is understandable from a colloidal point of view[32] since the extra water-shedding tail in ADG is expected to enhance a cooperative assembly behavior in analogy to membrane lipids. The two-state conversion observed with ADG may occur either through an intermediate molecular species with a mixed secondary structure within each individual peptide, or as a mixture of two peptides with different secondary structures.[33] Other methods than CD are required to distinguish between these intra- and intermolecular scenarios.

In contrast to ADG/AD both AKG and ARG fail to form a typical characteristic of β-sheet spectrum in water even at high concentration (Fig. 3b,c). The changed ellipticities per residue between 0.1 and 0.8 mM indicate that the secondary structures of AKG and ARG are still sensitive to peptide concentration. For AKG a CONTIN analysis suggests that the secondary structure converts from α-helix at low concentration to unordered at high.

For ARG the conversion is more complicated, but may still occur by a transition from α-helix to unordered.[34,35]

Effect of pH on charge and secondary structure. Both ADG and AD contain less amount of β-structure as pH is increased from 4 to 9.5 (Fig. 5a,d), whereas both AKG and ARG obviously exhibit a β-sheet type of structure throughout this pH-range (Fig. 5b,c). An important conclusion from these pH effects is that the amount of β-sheet in the double-tail peptides decreases as the peptide charge increases (Fig. S2†).

Peptide aggregation in water. The individual double-tail peptides are 2–5 nm long (Table 1), but the DLS data (Table 1) show that the structures the peptides form in water have average hydrodynamic sizes between ten and hundreds of nanometres. So clearly the peptide building blocks in Scheme 1 interact in water, forming supramolecular aggregates with a wide range of sizes. The nature of the size distributions (Fig. 7) suggests that the outcome of the aggregation depends on both the number of tails and the chemical nature of the head. The size distribution is bimodal for double-tailed ADG but monomodal for the single-tail control AD (Fig. 7), and it is bimodal for ARG but monomodal for AKG even though both these peptides have the same +2 head charge and only differ in the chemical nature of the side-chains of the head. The colloidal properties of the double-tail peptides in pure water will be investigated in a separate study. For the present purpose (self-assembly in the presence of added salt), it suffices to conclude that Fig. 7 evidences that the two-tail peptides form supramolecular aggregates in aqueous solutions.

B. Peptide behavior in salt solutions

Turning to salt-solutions, we ask two questions: how does the increased ionic strength affect the secondary structure of the building blocks, and which nanostructures are formed by self-assembly in the presence of added salt.

Effect of added salt on the secondary structure. The experiments in Fig. 8 were intended to probe the secondary structures in our protocol for salt-induced self-assembly. Adding salt like PBS or NaCl has weak effects on the secondary structures of AKG and ARG when compared to water (Fig. 8b,c), which supports that these two peptides are quite insensitive to external conditions including peptide concentration (Fig. 3), pH (Fig. 5) and temperature (Fig. 6). Adding PBS to ADG and AD remove their β-sheet structure altogether (Fig. 8a,d) as expected from Fig. 5. The pH of 7.2 will lead to full dissociation of the Asp-heads (ESI†) which counteracts β-sheet formation by electrostatic repulsion. When salt is added in the form of (unbuffered) NaCl the pH will not be affected, and the primary effect of added salt is expected to be a screening of the electrostatic interactions. However, electrostatic effects will be weaker than in PBS since the charge fraction at the final 0.2 mM peptide concentration is estimated to be only 0.5 (see ESI†). Indeed, with AD there is no effect of the NaCl on the secondary structure, and with ADG (Fig. 8d) the effect on the β-sheet type of spectrum is weaker than in PBS. In conclusion, increasing the ionic strength by adding NaCl seems to have small or no effect on the secondary structure of the peptide building blocks.

Effect of added salt on the self-assembly process. One goal here was to understand how the supra-molecular structures, as observed by AFM (Fig. 9), are influenced by the primary structure of the peptides (Table 1), perhaps indirectly through the secondary structures as monitored by CD in the relevant solvents (Fig. 3–5 and 8).

The 0.25 mM peptide concentration used in the AFM-studies (Fig. 9) is lower than the 0.8 mM concentration typically needed to form a stable secondary structure in water (Fig. 3), but significantly higher than the 0.01 M concentration at which the CD-results suggest that peptides act as individual molecules (Fig. 4). The self-assembly thus occurs at concentrations where the peptides interact, and this observation begs the question what drives the peptides to come together.

Comparing AFM-images in 0.1 M NaCl and pure water (Fig. 9) clearly shows that self-assembly requires the presence of salt. One possibility is that the added salt affects peptide interactions indirectly by changing their secondary structure, but the CD spectra with and without NaCl (Fig. 8) indicate that this effect is not a major one (except may be for ADG). A more likely role of the added salt is a direct promotion of peptide–peptide interactions by screening of electrostatic interactions. The interaction will certainly be repulsive since the peptides were designed to be purely negative (ADG) or positive (AKG/ARG), and screening will be important since the protolytic groups are charged to more than 40% at the concentrations typically used in AFM (see Fig. S3†).

One may ask how these new simple amphiphilic peptides could form such well-ordered nanofibers and nanolayers. The understanding of these processes as to structural details is still far from complete, but previous results on designed self-assembling peptide recapitulates the key elements of chemical complementarity and structural compatibility.[5] Weak inter-molecular interaction (hydrogen and ionic bonds, hydrophobic and van der Waals interactions) play important roles in molecular self-assembly. The self-assembling process integrates intrinsic and extrinsic factors[2,31,33,36,39–41] such as the primary amino acid sequence, the size and concentration of the peptide, as well as the pH, temperature and ionic strength, of the solvent. For instance, the formation of nanofibers has been ascribed to the presence of a β-sheet precursor.[5] Apart from ARG, the present set of data (Fig. 8 and 9) confirms this prediction since both ADG and AD exhibit a characteristic β-sheet spectrum (minimum 216 nm, maximum 204 nm) and form nanofibers, while AKG is not β-sheet and self-assemble into nano-layers (Fig. 9b). ARG forms nanofibers under AFM-conditions (Fig. 9c) which is unexpected since the secondary structure is not a characteristic of β-sheet spectrum (minimum 217 nm, maximum 204 nm). Clearly more experiments are needed to understand the relation between primary structures of double-tail peptides and the supra-molecular assemblies they form under various solvent conditions.

The two-tail peptides differ from most lipids,[6,7,9] in that the peptides have tails that can interact by intermolecular hydrogen bonding in addition to hydrophobic interactions. Thus, some peptides such as ADG and AD displayed typical characteristic β-sheet structures, and their tails are likely packed in the β-sheet manner but with a certain curvature due to the repulsion between negative charged heads. Other peptides like AKG and ARG show CD spectra that could indicate an unordered structure, the

tails kept apart by the repulsion of positive charges. Further insight into the detailed mechanisms of the aggregation process is needed, in particular about the roles of water-mediated hydrogen bonds as these peptide molecules interact on many points with water, in contrast to classical amphiphilic molecules. More evidence regarding the role of β-sheet stabilisation for the self-assembling into well ordered nanostructures is also desirable.

C. Potential applications to biomedical and nanobiotechnology engineering

Bottom-up strategies using self-assembling peptides with alternating ionic and amphiphilic amino acids and produce nanofiber scaffolds can have interesting applications in various areas, including cell engineering,[30,42] tissue repair and tissue regeneration,[43,44] haemostatic strategy for stopping bleeding as well as slow drug release,[28] or peptides for gene delivery resistant to natural proteases.[41]

Our results indicate that among this new kind of amphiphilic peptides, ARG and AKG form robust aggregates with secondary structures that are stable over a wide range of concentrations, temperatures, pHs and salts. We have shown how these peptides can self-assemble to particular nanostructures such as nanofibers or nanolayers, and we anticipate these systems to be versatile for a broad spectrum of applications compared to the previously studied one-tail amphiphilic peptides, the here further developed peptides carrying double tails may be designed and modified for a variety of uses. For example, these molecules made of L-amino acids that can be degraded and recycled in the body, if designed with excess of positive charge may compact or encase negatively charged nucleic acids for gene delivery or delivery of siRNA, thereby potentially providing efficient, nontoxic, non-immunogenic transfection and cell-penetrating agents. We also note that with one hydrophobic and one hydrophilic tail the peptides may find use as "super-surfactants" to stabilize membrane proteins, either in biomedical context or for structural studies in solution or crystal state.

Conclusions

To summarize the results in water (no added salt), the three double-tail peptides form supramolecular aggregates with wide and non-trivial size distributions. The secondary structure of ADG is β-sheet, formed in a two-state process from the individual building blocks and controllable by pH. The secondary structure of AKG and ARG is stable in a wide range of pHs and temperatures, but unknown in the sense it is neither β-sheet nor α-helix. The new type of molecularly engineered peptides with double tails may find a range of applications to meet demands of a growing biomedical and emerging nanobiotechnology, including use for unimolecular handling of membrane proteins, construction of nano-devices/nano-machines, or for drug formulation/delivery or gene therapy.

Acknowledgements

BN acknowledges funding from the King Abdullah University of Science and Technology (KAUST). BÅ acknowledges a grant from the Swedish Research Council. Johan Bergenholtz is thanked for assistance in the DLS measurements. ZL thanks Per Lincoln, Niklas Bosaeus and Johanna Andersson for assistance and helpful discussions.

References

1 S. Liao and N. C. Seeman, *Science*, 2004, **306**, 2072–2074.
2 S. Zhang, T. Holmes, C. Lockshin and A. Rich, *Proc. Natl. Acad. Sci. U. S. A.*, 1993, **90**, 3334–3338.
3 H. Yan, S. H. Park, G. Finkelstein, J. H. Reif and T. H. LaBean, *Science*, 2003, **301**, 1882–1884.
4 J. Tumpane, R. Kumar, E. P. Lundberg, P. Sandin, N. Gale, I. S. Nandhakumar, B. Albinsson, P. Lincoln, L. M. Wilhelmsson, T. Brown and B. NordÁn, *Nano Lett.*, 2007, **7**, 3832–3839.
5 S. Zhang, *Nat. Biotechnol.*, 2003, **21**, 1171–1178.
6 S. Vauthey, S. Santoso, G. Haiyan, N. Watson and S. Zhang, *Proc. Natl. Acad. Sci. U. S. A.*, 2002, **99**, 5355.
7 S. Santoso, W. Hwang, H. Hartman and S. Zhang, *Nano Lett.*, 2002, **2**, 687–691.
8 G. v. Maltzahn, S. Vauthey, S. Santoso and S. Zhang, *Langmuir*, 2003, **19**, 4332–4337.
9 A. Nagai, Y. Nagai, H. Qu and S. Zhang, *J. Nanosci. Nanotechnol.*, 2007, **7**, 1–7.
10 K. Hayakawa, J. P. Santerre and J. C. T. Kwak, *Biophys. Chem.*, 1983, **17**, 175–181.
11 B. W. Pontius and P. Berg, *Proc. Natl. Acad. Sci. U. S. A.*, 1991, **88**, 8237–8241.
12 S. M. Mel'nikov, V. G. Sergeyev and K. Yoshikawa, *J. Am. Chem. Soc*, 1995, **117**, 9951–9956.
13 V. Budker, V. Gurevich, J. E. Hagstrom, F. Bortzov and J. A. Wolff, *Nat. Biotechnol.*, 1996, **14**, 760–764.
14 O. Zelphati and J. F. C. Szoka, *Proc. Natl. Acad. Sci. U. S. A.*, 1996, **93**, 11493–11498.
15 I. Koltover, T. Salditt, J. O. Rädler and C. R. Safinya, *Science*, 1998, **281**, 78–81.
16 R. A. D. S. Strayer, B. A. Bunnell, B. Dropulic, V. Planelles, R. J. Pomerantz, J. J. Rossi and J. A. Zaia, *Mol. Ther.*, 2005, **11**, 823–842.
17 H. Åmand, K. Fant, B. Nordén and E. Esbjörner, *Biochem. Biophys. Res. Commun.*, 2008, **371**, 621–625.
18 E. K. Esbjörner, K. Oglecka, P. Lincoln, A. Gräslund and B. Nordén, *Biochemistry*, 2007, **46**, 13490–13504.
19 L. Kaiser, J. Graveland-Bikker, D. Steuerwald, M. I. Vanberghem, K. Herlihy and S. Zhang, *Proc. Natl. Acad. Sci. U. S. A.*, 2008, **105**, 15726–15731.
20 B. L. Cook, K. E. Ernberg, H. Chung and S. Zhang, *PLoS One*, 2008, **3**, e2920.
21 P. Kiley, X. Zhao, M. Vaughn, M. A. Baldo, B. D. Bruce and S. Zhang, *PLoS Biol.*, 2005, **3**, 1180–1186.
22 X. Zhao, Y. Nagai, P. J. Reeves, P. Kiley, H. G. Khorana and S. Zhang, *Proc. Natl. Acad. Sci. U. S. A.*, 2006, **103**, 17707–17712.
23 G. Wada and T. Takenaka, *Bull. Chem. Soc. Jpn.*, 1971, **44**, 2877.
24 B. Noszál and R. Kassai-Tánczos, *Talanta*, 1991, **38**, 1439–1444.
25 C. R. Cantor and P. R. Schimmel, *Biophysical Chemistry, Part II: techniques for the Study of Biological Structure and Function*, W.H. Freeman and Co., New York, 1980.
26 L. Whitmore and B. A. Wallace, *Biopolymers*, 2007, **89**, 392–400.
27 A. Rodger and B. Nordén, in *Circular Dichroism and Linear Dichroism*, ed. A. Rodger, B. Nordén, Oxford University Press, New York, 1997.
28 C. Keyes-Baig, J. Duhamel, S.-Y. Fung, J. Bezaire and P. Chen, *J. Am. Chem. Soc.*, 2004, **126**, 7522–7532.
29 S. Zhang, *Biotechnol. Adv.*, 2002, **20**, 321.
30 S. Zhang, T. Holmes, M. DiPersio, R. O. Hynes, X. Su and A. Rich, *Biomaterials*, 1995, **16**, 1385–1393.
31 Z. Luo, X. Zhao and S. Zhang, *PLoS One*, 2008, **3**, e2364.
32 D. F. Evans and H. Wennerstrom, *The Colloidal Domain: where Physics, Chemistry and Biology Meet*, WileyBlackwell, New York, 2nd edn 1999.
33 M. Altman, P. Lee, A. Rich and S. Zhang, *Protein Sci.*, 2000, **9**, 1095–1105.
34 L. Whitmore and B. A. Wallace, *Biopolymers*, 2008, **89**, 392–400.
35 L. Whitmore and B. A. Wallace, *Nucleic Acids Res.*, 2004, **32**, 668–673.
36 S. Zhang and A. Rich, *Proc. Natl. Acad. Sci. U. S. A.*, 1997, **94**, 23.

37 J. P. Greenstein, *J. Biol. Chem.*, 1931, **93**, 479–494.
38 E. Ellenbogen, *J. Am. Chem. Soc.*, 1952, **74**, 5198–5201.
39 Y. Hong, R. L. Legge, S. Zhang and P. Chen, *Biomacromolecules*, 2003, **4**, 1433–1442.
40 H. Yokoi, T. Kinoshita and S. Zhang, *Proc. Natl. Acad. Sci. U. S. A.*, 2005, **102**, 8414–8419.
41 Z. Luo, X. Zhao and S. Zhang, *Macromol. Biosci.*, 2008, **8**, 785–791.
42 F. Gelain, A. Lomander, A. L. Vescovi and S. Zhang, *PLoS One*, 2006, **1**, e119.
43 J. Kisiday, M. Jin, B. Kurz, H. Hung, C. Semino, S. Zhang and A. J. Grodzinsky, *Proc. Natl. Acad. Sci. U. S. A.*, 2002, **99**, 9996–10001.
44 G. R. Ellis-Behnke, Y. -X. Liang, D. K. C. Tay, P. W. F. Kau, G. E. Schneider, S. Zhang, W. Wu and K.-F. So, *Nanomed.: Nanotechnol. Biol. Med.*, 2006, **2**, 207–215.

